

## Asymptotic analysis and effect of reaction order on a reversible gas–solid system with fast reaction

Y.H. CHAN<sup>1</sup> and D.L.S. McELWAIN

<sup>1</sup>School of Mathematics, Queensland University of Technology, GPO Box 2434 Brisbane, Queensland 4001, Australia and Department of Mathematics, The University of Newcastle, Callaghan, NSW 2308, Australia

Accepted 16 November 1992; accepted in revised form 21 June 1995

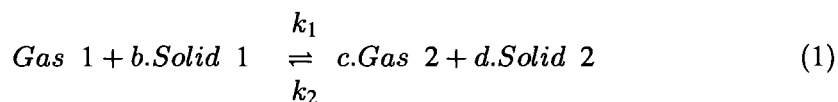
**Abstract.** The development of approximate methods for the equations describing noncatalytic reversible gas–solid systems with fast reactions are investigated by means of perturbation techniques and series solutions. The effect of the reaction orders, when the back reaction is not neglected, on the existence of a moving boundary is also discussed. It is shown that a moving boundary exists only when the reversible reaction rate is independent of the reactant solid concentration.

Estimates for conversion times are also obtained for the cases where all the reaction orders are non–zero and where the kinetics is independent of the reactant and product solids. These approximate solutions may find application, for example, in computational models of ironmaking blast furnaces.

### 1. Introduction and formulation

Over the years, a number of mathematical models have been introduced in the theoretical analysis of the gas–solid reactions which find important applications in metallurgical and chemical manufacturing processes. Practical situations are given, for example, in Ramachandran and Doraiswamy [1] and Sampath and Hughes [2]. Basically, these models can be categorised into two main classes, one in which there exists a moving boundary and the other without. The former class consists of the well–known shrinking core model, as discussed in Levenspiel [3] and Szekely *et al* [4], which rests on the assumption that the reaction is localised at an interface (or a very narrow zone) between the completely unreacted core and the completely reacted product layer. This is true when the reaction rate is very rapid compared with the diffusion of the reactant gas, as shown by Do [5], or when the solid reactant is nonporous, a case discussed by Levenspiel [3]. The other circumstance in which there is a moving boundary, the reaction zone is diffuse throughout the solid ensemble with the concentration of the solid reactant falling gradually to zero at that interface (Ishida and Wen [6]). Generally, the above models have been analysed neglecting the back reaction or if it is included, the reaction rates are assumed to be of first order in both reactant and product gases and independent of the solid concentrations, as illustrated in the papers by McAdam *et al* [7] and Szekely *et al* [4].

We consider an isothermal reversible noncatalytic gas–solid system represented by



in which solid 1 is converted to solid 2. We assume that there is no change in the particle's size during the course of reaction and that the solids do not diffuse. Then the material balance

equations are given by

$$\varrho \frac{\partial G'_1}{\partial t'} = D_1 \nabla_{x'}^2 G'_1 - f' \quad (1.1)$$

$$\frac{\partial S'_1}{\partial t'} = -bf' \quad (1.2)$$

$$\varrho \frac{\partial G'_2}{\partial t'} = D_2 \nabla_{x'}^2 G'_2 + cf' \quad (1.3)$$

$$\frac{\partial S'_2}{\partial t'} = df' \quad (1.4)$$

where  $\nabla_{x'}^2 = x'^{-\alpha} \frac{\partial}{\partial x'} (x'^{\alpha} \frac{\partial}{\partial x'})$  with  $\alpha = 0, 1, 2$  for slab, cylindrical and spherical geometries respectively.

In the above equations,  $G'_1$  and  $G'_2$  are the concentrations of the reactant and product gases, respectively. Similarly  $S'_1$  and  $S'_2$  are that of the solids.  $D_1$  and  $D_2$  are the respective diffusion coefficients, assumed to be constant, for the reactant and product gases. The parameter  $\varrho$ , assumed to be constant, is the porosity. The constants  $b$ ,  $c$  and  $d$  are the stoichiometric coefficients. We assume power-law kinetics so that  $f'$ , the total reaction rate, is given by

$$f' = k_1 G_1'^{n_1} S_1'^{m_1} - k_2 G_2'^{n_2} S_2'^{m_2} \quad (1.5)$$

where  $k_1$  and  $k_2$  are the forward and back reaction rate constants respectively. The parameters  $n_1$ ,  $m_1$ ,  $n_2$  and  $m_2$  are the reaction orders of the reactant and product concentrations.

We assume that initially, the particle is wholly of type solid 1, of concentration  $S_0$ , having no gas of either type inside it and the reactant gas is supplied externally from an inexhaustible source of concentration  $G_0$ . We also assume that there is no gas film around the particle and symmetry is observed if the geometry of the particle is spherical or cylindrical, else half of a slab with width  $2L$  is considered. Thus, the initial and boundary conditions are given by

$$t' = 0, \quad G'_1 = G'_2 = S'_2 = 0, \quad S'_1 = S_0, \quad (1.6)$$

$$x' = 0, \quad \frac{\partial G'_1}{\partial x'} = \frac{\partial G'_2}{\partial x'} = 0, \quad (1.7)$$

and

$$x' = L, \quad G'_1 = G_0, \quad G'_2 = 0 \quad (1.8)$$

## 2. Non-dimensionalisation

We define the following non-dimensional parameters and variables :

$$G_1 = \frac{G'_1}{G_0} \quad S_1 = \frac{S'_1}{S_0} \quad x = \frac{x'}{L}$$

$$G_2 = \frac{G'_2}{G_0} \quad S_2 = \frac{S'_2}{S_0} \quad t = \frac{D_1 t'}{\varrho L^2}$$

$$\phi^2 = \frac{k_1 G_0^{n_1} S_0^{m_1} L^2}{D_1 G_0} \quad \psi = \frac{\rho G_0}{S_0} \quad K = \frac{k_1 G_0^{n_1 - n_2}}{k_2 S_0^{m_2 - m_1}} \quad \delta = \frac{D_2}{D_1}$$

then the non-dimensionalised material balance equations are

$$\frac{\partial G_1}{\partial t} = \nabla^2 G_1 - \phi^2 f \quad (2.1)$$

$$\frac{\partial S_1}{\partial t} = -\psi \phi^2 b f \quad (2.2)$$

$$\frac{\partial G_2}{\partial t} = \delta \nabla^2 G_2 + \phi^2 c f \quad (2.3)$$

$$\frac{\partial S_2}{\partial t} = \psi \phi^2 d f \quad (2.4)$$

where  $\nabla^2 = x^{-\alpha} \frac{\partial}{\partial x} (x^\alpha \frac{\partial}{\partial x})$  with  $\alpha = 0, 1, 2$  for slab, cylindrical and spherical geometries respectively and  $f$  is given by

$$f = G_1^{n_1} S_1^{m_1} - \frac{1}{K} G_2^{n_2} S_2^{m_2}$$

where  $K$  is the equilibrium constant. This power-law type kinetics has been widely assumed in the analysis of gas–solid reactions. For example, in the case of irreversible reactions ( $K \gg 1$ ), Borghi *et al* [8], Dudukovic [9] and Stakgold and McNabb [10] assumed a first order in the reactant gas but arbitrary order in the reactant solid. For the situation of reversible kinetics, as mentioned above, McAdam *et al* [7] and Szekely *et al* [4] assumed that the kinetics were independent of the solid concentrations.

The dimensionless time is based on the characteristic diffusion time of the reactant gas. The dimensionless parameter,  $\phi$ , is the Thiele Modulus. It is the ratio of the characteristic time for diffusion,  $L^2/D_1$ , to that of the reaction characteristic time  $G_0/(k_1 G_0^{n_1} S_0^{m_1})$ . It therefore measures the relative importance of the diffusion of the reactant gas to reaction phenomena. For example, if  $\phi$  is large, the reaction rate is fast compared to the diffusion of the reacting gas.

The dimensionless parameter,  $\psi$ , is the ratio of the bulk gas and the initial solid concentration. This parameter is usually much less than unity for gas–solid reactions. The dimensionless parameter,  $\delta$ , is the ratio of the characteristic diffusion times of the diffusing gas  $G_1$ ,  $\rho L^2/D_1$ , to that of the product gas  $G_2$ ,  $\rho L^2/D_2$ . If  $\delta$  is small, the product gas will take a longer time to diffuse out of the particle.

The transformed initial and boundary conditions are given by

$$t = 0, \quad G_1 = G_2 = S_2 = 0, S_1 = 1 \quad (2.5)$$

$$x = 0, \quad \frac{\partial G_1}{\partial x} = \frac{\partial G_2}{\partial x} = 0 \quad (2.6)$$

$$x = 1, \quad G_1 = 1, G_2 = 0 \quad (2.7)$$

From equations (2.2), (2.4) and applying the initial conditions (2.5), we have an expression for the conservation of the solids, namely

$$dS_1 + bS_2 = d. \quad (2.8)$$

We see that the final state associated with these boundary conditions is the complete conversion of the solid  $S_1$ . We thus have  $G_1 = 1$ ,  $G_2 = 0$  and  $S_1 = 0$  as the ultimate state of this system.

In this work, by means of perturbation techniques and series solutions (by separation of variables), we carry out an analysis on an isothermal reversible noncatalytic gas-solid system under the assumption that the reaction rate is very rapid compared with the rate of diffusion of the gaseous reactant ( $\phi \gg 1$ ). We also assume that the parameter  $\psi$  is small and the parameter  $\delta$  to be of order unity. The effect of the reaction orders on the existence of a moving boundary is also presented. Estimates for conversion times for the case where all the reaction orders are non-zero and also the case where the kinetics is independent of the reactant and product solid concentrations are discussed.

### 3. Transient period

From equations (2.1-2.4), we see that in the initial transient period, the time-derivative terms can take part in a dominant balance only if we rescale the time and introduce a short time scale  $t^+$  where, for  $\phi^2 \gg 1$ ,

$$t^+ = \phi^2 t.$$

Then equations (2.1-2.4) become

$$\frac{\partial G_1}{\partial t^+} = \mu^2 \nabla^2 G_1 - f \quad (3.1)$$

$$\frac{\partial S_1}{\partial t^+} = -\psi b f \quad (3.2)$$

$$\frac{\partial G_2}{\partial t^+} = \delta \mu^2 \nabla^2 G_2 + c f \quad (3.3)$$

$$\frac{\partial S_2}{\partial t^+} = \psi d f \quad (3.4)$$

with initial and boundary conditions given by equations (2.5-2.7) with  $t$  replaced by  $t^+$  and  $\mu = \frac{1}{\phi} \ll 1$ .

Firstly, we seek a straightforward asymptotic expansion in the form,

$$G_i = G_i^0 + \mu^2 G_i^1 + \dots$$

$$S_i = S_i^0 + \mu^2 S_i^1 + \dots$$

for  $i=1,2$ . Substituting into equations (3.1-3.4) gives the leading order

$$\frac{\partial G_1^0}{\partial t^+} = -f^0 \quad (3.5)$$

$$\frac{\partial S_1^0}{\partial t^+} = -\psi b f^0 \quad (3.6)$$

$$\frac{\partial G_2^0}{\partial t^+} = c f^0 \quad (3.7)$$

$$\frac{\partial S_2^0}{\partial t^+} = \psi df^0 \quad (3.8)$$

where

$$f^0 = G_1^{0n_1} S_1^{0m_1} - \frac{1}{K} G_2^{0n_2} S_2^{0m_2}$$

and the initial conditions are given by

$$t^+ = 0, \quad G_1^0 = G_2^0 = S_2^0 = 0, \quad S_1^0 = 1$$

Solving equations (3.5-3.8) gives the *undisturbed* region (outer solution) in the domain  $0 \leq x < 1$ , that is

$$G_1^{out} = G_2^{out} = S_2^{out} = 0, \quad S_1^{out} = 1 \quad (3.9)$$

By examining the conditions (2.7) and (3.9) for  $G_1$ , we see that large spatial gradients are expected to occur near  $x = 1$  and to analyse this boundary layer, we introduce the stretched variable  $\zeta$  as

$$\zeta = \frac{1-x}{\mu}$$

Then in terms of  $\zeta$ , equations (3.1-3.4) become

$$\frac{\partial G_1}{\partial t^+} = \frac{\partial^2 G_1}{\partial \zeta^2} - f \quad (3.10)$$

$$\frac{\partial S_1}{\partial t^+} = -\psi b f \quad (3.11)$$

$$\frac{\partial G_2}{\partial t^+} = \delta \frac{\partial^2 G_2}{\partial \zeta^2} + c f \quad (3.12)$$

$$\frac{\partial S_2}{\partial t^+} = \psi d f \quad (3.13)$$

with the initial and boundary conditions given by

$$t^+ = 0, \quad G_1 = G_2 = S_2 = 0 \quad S_1 = 1 \quad (3.14)$$

$$\zeta = 0, \quad G_1 = 1 \quad G_2 = 0 \quad (3.15)$$

$$\zeta \rightarrow \infty, \quad G_1 = G_2 = S_2 = 0 \quad S_1 = 1 \quad (3.16)$$

### Structure for $t^+ \ll 1$

To observe the manner in which the solutions of equations (3.10–3.16) evolve initially, we examine the limit as  $t^+ \rightarrow 0$ . We assume a perturbation expansion for the  $G$ 's and  $S$ 's in the layer (inner solution) near the outer edge of the particle, as discussed by Aziz and Na [11] and Kapila [12], in the form

$$G_i^{in} = \sum_{p=0}^{\infty} \tau^p G_{ip}(\eta)$$

$$S_i^{in} = \sum_{p=0}^{\infty} \tau^p S_{ip}(\eta)$$

for  $i = 1, 2$ ,  $\eta = \frac{\zeta}{2\sqrt{t^+}}$  and  $\tau = 4t^+$ . Substituting these series into equations (3.10–3.13) and equating coefficients of  $\tau^0$  gives the following results:

$$G_{10} = \operatorname{erfc} \eta, \quad S_{10} = 1, \quad G_{20} = S_{20} = 0 \quad (3.17)$$

where *erfc* is the complimentary error function. To this order of approximation, the initial behaviour of the system involves only the diffusion of the reactant gas with no reaction and thus no product gas or solid conversion. This result is similar to that found by Kapila [12] in a system which models the reaction and diffusion of two diffusing species with no back reaction.

From the results obtained in (3.17), we can assume that at this very short time scale  $t^+$ , the reactant solid  $S_1$  is of order unity, then with  $S_1 = 1$ , equation (3.10) reduces to

$$\frac{\partial G_1}{\partial t^+} = \frac{\partial^2 G_1}{\partial \zeta^2} - G_1^{n_1} \quad (3.18)$$

with the initial and boundary conditions given by

$$t^+ = 0, \quad G_1 = 0 \quad (3.19)$$

$$\zeta = 0, \quad G_1 = 1 \quad (3.20)$$

$$\zeta \rightarrow \infty, \quad G_1 = 0 \quad (3.21)$$

We now discuss and investigate exact/approximate solutions for equations (3.18–3.21).

#### A. KNOWN EXACT SOLUTIONS

Carslaw and Jaeger [13] used equations (3.18–3.21), with  $n_1 = 1$ , to describe the conduction of heat along a thin rod which loses heat from its periphery at a rate proportional to its temperature, and the exact solution is given by,

$$G_1^e = \frac{1}{2} e^{-\zeta} \operatorname{erfc} \left[ \frac{\zeta}{2\sqrt{t^+}} - \sqrt{t^+} \right] + \frac{1}{2} e^{\zeta} \operatorname{erfc} \left[ \frac{\zeta}{2\sqrt{t^+}} + \sqrt{t^+} \right]. \quad (3.22)$$

When  $n_1 \neq 1$ , closed form expressions for  $G_1$  are not available.

#### B. PERTURBATION EXPANSIONS

Equation (3.18) has also been used to describe the temperature response of fins by Aziz and Na [11]. They gave a fourth order perturbation solution with  $n_1 = 1$ , and we can use this to obtain an approximation to the reactant gas concentration  $G_1$ , namely,

$$G_1^p = \sum_{i=0}^4 \tau^i \theta_i$$

with

$$\theta_0 = \operatorname{erfc} \eta$$

$$\theta_1 = i^2 \operatorname{erfc} \eta - \frac{1}{4} \operatorname{erfc} \eta$$

$$\begin{aligned}\theta_2 &= i^4 \operatorname{erfc} \eta - \frac{1}{4} i^2 \operatorname{erfc} \eta + \frac{1}{32} \operatorname{erfc} \eta \\ \theta_3 &= i^6 \operatorname{erfc} \eta - \frac{1}{4} i^4 \operatorname{erfc} \eta + \frac{1}{32} i^2 \operatorname{erfc} \eta - \frac{1}{384} \operatorname{erfc} \eta \\ \theta_4 &= i^8 \operatorname{erfc} \eta - \frac{1}{4} i^6 \operatorname{erfc} \eta + \frac{1}{32} i^4 \operatorname{erfc} \eta - \frac{1}{384} i^2 \operatorname{erfc} \eta + \frac{1}{6144} \operatorname{erfc} \eta\end{aligned}$$

where  $p$  denotes an approximation based on a perturbation expansion.

For  $n_1$  not unity, Aziz and Na [11] mention that closed form solutions do not appear to be available and Na [14] has outlined in detail a *Method of Superposition* to provide the numerical solutions.

We can also obtain an expression for the product gas concentration. For the special case of  $\delta = 1$  and  $n_1 = 1$ , the solutions for  $G_2$  are given by

$$G_2^p = -c \sum_{i=1}^4 \tau^i \theta_i$$

where the  $\theta_i$  are given above. For the case of arbitrary  $\delta$ , closed form solutions are only available for the first order perturbation, namely,

$$G_2^p = \tau \operatorname{erfc} \sqrt{\frac{\eta}{\delta}}$$

Finally, with  $n_1 = 1$ , the reactant solid (only using a second order perturbation) is given by

$$S_1^p = 1 + \sum_{i=1}^2 \tau^i \gamma_i$$

where

$$\gamma_1 = \psi b \left[ \frac{1}{2\sqrt{\pi}} \eta e^{-\eta^2} - \frac{\eta^2}{2} \operatorname{erfc} \eta - \frac{1}{4} \operatorname{erfc} \eta \right]$$

$$\gamma_2 = \psi b \left[ \frac{1}{8} I_1 - \frac{1}{2} I_2 \right]$$

with

$$I_1 = \frac{1}{4} \operatorname{erfc} \eta - \frac{\eta}{6\sqrt{\pi}} e^{-\eta^2} + \frac{\eta^3}{3\sqrt{\pi}} e^{-\eta^2} - \frac{1}{3} \eta^4 \operatorname{erfc} \eta$$

$$I_2 = \frac{1}{4} i^2 \operatorname{erfc} \eta - \frac{\eta}{12} i \operatorname{erfc} \eta + \frac{1}{24} \eta^2 \operatorname{erfc} \eta - \frac{1}{12\sqrt{\pi}} \eta^3 e^{-\eta^2} + \frac{1}{12} \eta^4 \operatorname{erfc} \eta$$

Then from the expression for the conservation of the solids, we get

$$S_2^p = \frac{d}{b} (1 - S_1^p)$$

Results for the case of spherical geometry with  $\phi = 100$ ,  $\psi = 0.1$  and all other parameters being unity are presented in Figure 1. The above solutions also provide good results for slab and cylindrical geometries.

As can be seen from Figure 1, the method developed in this section provides excellent approximations to the distributions for all species when  $t^+$  is small ( $t^+ \leq 2$ ).

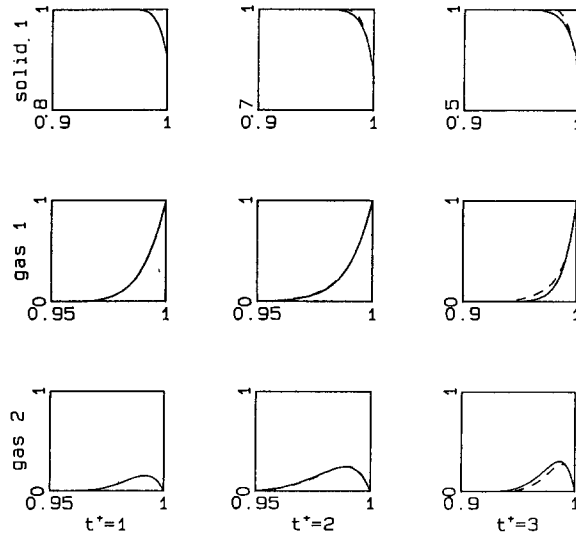


Fig. 1. Distributions obtained from a full numerical solution (—) for a sphere with  $\phi = 100$ ,  $\psi = 0.1$  and other parameters unity (this work : - - - - Results from the Perturbation Approximation).

C. SERIES SOLUTIONS

As an alternative to the perturbation procedure described above, if  $0 < \mu \ll 1$ , equations (3.18–3.21) can also be solved in terms of series solutions, with the boundary condition (3.21) replaced by

$$\zeta = \frac{1}{\mu}, \quad \frac{\partial G_1}{\partial \zeta} = \frac{\partial G_2}{\partial \zeta} = 0$$

For the case of  $n_1 = 1$  we have,

$$G_1^s = e^{-\zeta} - \sum_{p=1}^{\infty} 2\mu \frac{\xi_1}{\lambda_1^2} \sin(\xi_1 \zeta) e^{-\lambda_1^2 t^+} \tag{3.23}$$

where

$$\xi_1 = (2p - 1) \frac{\mu\pi}{2} \quad p = 1, 2, \dots \quad \text{with } \lambda_1^2 = \xi_1^2 + 1$$

and  $s$  denotes an approximation based on a series solution. The solutions described by expressions (3.22) and (3.23) give extremely similar results.

One advantage of using the series solution rather than the exact or perturbation expressions is that simple results for the reactant solid and product gas concentrations can be easily obtained. Since on this *fast* time scale, the back reaction remains negligible, using the series



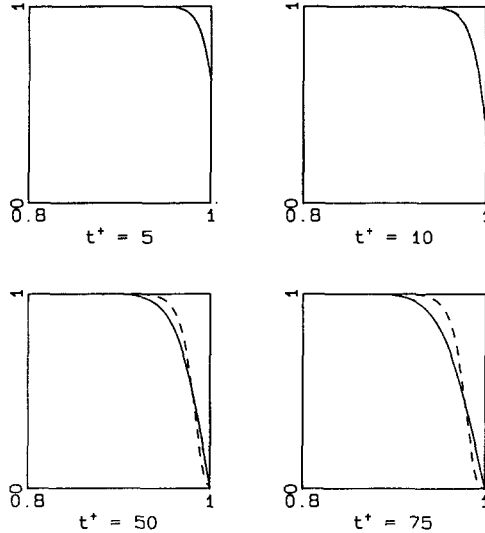


Fig. 2. Results obtained from full numerical solution (——) for a sphere with  $\phi = 100$ ,  $\psi = 0.1$  and other parameters unity (this work : - - - - Results for the series method).

expansions, the reactant solid concentration is given by

$$S_1^s = \begin{cases} e^{-\psi b \left[ e^{-\zeta t^+} + \sum_{p=1}^{\infty} \frac{2\mu\xi_1}{\lambda_1^4} \sin(\xi_1\zeta) [e^{-\lambda_1^2 t^+} - 1] \right]}, & m_1 = 1, \\ \left[ 1 - \psi b(1 - m_1) \left[ e^{-\zeta t^+} + \sum_{p=1}^{\infty} \frac{2\mu\xi_1}{\lambda_1^4} \sin(\xi_1\zeta) [e^{-\lambda_1^2 t^+} - 1] \right] \right]^{\frac{1}{1-m_1}}, & m_1 \neq 1. \end{cases} \quad (3.24)$$

Expanding equation (3.24) and gathering leading terms, we find that the solutions for  $S_1^s$  breakdown when  $t^+ \sim O\left(\frac{1}{b\psi}\right)$  for  $m_1 = 1$  and  $t^+ \sim O\left(\frac{1}{[1 - m_1]b\psi}\right)$  for  $m_1 \neq 1$ .

Figure 2 shows results obtained from expression (3.24) together with the numerical solution having all reaction orders being unity. Although with  $b = 1$  and  $\psi = 0.1$  we would expect the approximation to breakdown when  $t^+ \simeq 10$ , the approximation appears to be quite good up to  $t^+ = 25$ .

To obtain an estimate of the product gas concentration, since  $\psi$  is small, we use the steady state solution of  $G_1^s$  as the source term in the product gas equation, and get

$$G_2^s = \frac{c}{\delta} \left[ 1 - e^{-\zeta} + \sum_{p=1}^{\infty} 2\mu \left[ \frac{\xi_2}{\xi_2^2 + 1} + \frac{1}{\xi_2^2} \sin\left(\frac{\xi_2}{\mu}\right) - \frac{1}{\xi_2} \right] \sin(\xi_2\zeta) e^{-\lambda_2^2 t^+} \right] \quad (3.25)$$

where

$$\xi_2 = (2p - 1) \frac{\mu\pi}{2} \quad p = 1, 2, \dots \quad \text{with } \lambda_2^2 = \delta\xi_2^2$$

giving  $G_2^s(x, t^+) \geq G_2(x, t^+)$ . Results for the case of spherical geometry with  $\phi = 100$ ,  $\psi = 0.1$  and all other parameters being unity are presented in Figure 3. We would expect better results as  $\psi$  gets smaller.

Comparison of Figures 1 and 3 shows that while the perturbation solution provides a good approximation for short times, the series method gives excellent approximations for longer times. Another advantage of using the series solution technique is that for arbitrary  $n_1$ , bounds can be generated utilising the method discussed in our earlier work, Chan and McElwain [15], rather than solving equation (3.18) numerically.

STRUCTURE FOR  $t^+ \gg 1$

As  $t^+$  increases, the above results for the transient period will eventually breakdown. A new structure is required and following Kapila [12], we assume a perturbation expansion of the form, for  $i = 1, 2$ ,

$$G_i^{in} = \sum_{p=0}^{\infty} \frac{1}{\tau^p} \hat{G}_{ip}(\eta)$$

$$S_i^{in} = \sum_{p=0}^{\infty} \frac{1}{\tau^p} \hat{S}_{ip}(\eta)$$

where  $\eta = \frac{\zeta}{2\sqrt{t^+}}$  and  $\tau = 4t^+$ . Substituting these expansions into equations (3.10–3.13) shows that the leading order is governed by the reaction term,

$$\hat{G}_{10}^{n_1} \hat{S}_{10}^{m_1} - \frac{1}{K} \hat{G}_{20}^{n_2} \hat{S}_{20}^{m_2} = 0 \tag{4.1}$$

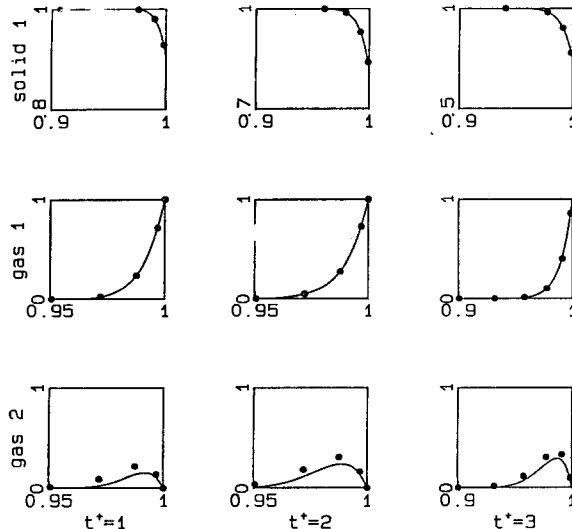


Fig. 3. Results obtained from full numerical solution (—) for a sphere with  $\phi = 100$ ,  $\psi = 0.1$  and other parameters unity (this work : • • Results for the series method).

Substituting the given boundary condition (2.7) into equation (4.1), we have

$$x = 1 \quad \hat{G}_{10} = 1, \quad \hat{G}_{20} = \hat{S}_{10} = 0, \quad \hat{S}_{20} = \frac{d}{b} \quad (4.2)$$

Thus, on this time scale, the reactant solid is completely reacted at the outer edge.

If  $K \gg 1$ , that is when the back reaction becomes insignificant, a sharp shrinking core is obtained as shown by Do [5]. Figure 4 shows numerical results of the effect of the equilibrium constant  $K$  on the solid distribution, with a certain set of the other parameters.

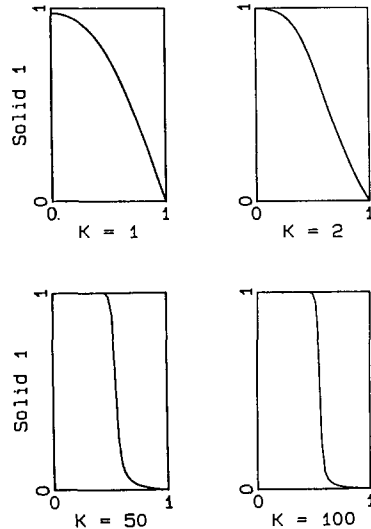


Fig. 4. Effect of equilibrium constant  $K$  for a slab geometry with  $\phi = 100$ ,  $\psi = 0.1$ ,  $t = 1.0$  and other parameters unity.

A perturbation analysis of the shrinking core model was first developed by Bischoff [16]. In that work, the perturbation expansion for the location of the moving boundary was neglected. Murray and Carey [17] used a moving finite–element technique to analyse the approximate solution of the shrinking core model having planar geometry. In a second paper, Carey and Murray [18], spherical geometry is considered and, utilising perturbation analysis and a finite–element formulation, the position of the interface is tracked precisely. Their results show that the error associated with Bischoff’s approximate perturbation model is small and thus vindicated its use. Do [5] showed that when the Thiele modulus is large and there is no back reaction, the shrinking core model is valid. Bhatia [19,20], performed a perturbation analysis on a general model having solid of low initial permeability. Both internal and external reactions are considered and the effect of the local internal conversion at the shrinking core is also taken into account. Bhatia showed that the diffusion–controlled form is a special case of internal reaction and diffusion, and that the most general form of the shrinking core model is obtained only when the reaction on the core surface is additionally considered.

In the above–mentioned papers, the back reaction has been neglected. When the back reaction is significant, with  $\phi$  large, we are interested to determine the effect of the parameters  $n_1$ ,  $m_1$ ,  $n_2$  and  $m_2$  on the existence of a moving boundary.

**4. Existence of shrinking core**Case 1 :  $n_1, m_1, n_2, m_2$  non-zero

We first consider the most general case where all the reaction orders are non-zero. From equation (2.8), we have  $\hat{S}_{20} = \frac{d}{b}(1 - \hat{S}_{10})$  and substituting this into equation (4.1) gives,

$$\hat{G}_{10}^{n_1} \hat{S}_{10}^{m_1} - \frac{1}{K} \hat{G}_{20}^{n_2} \left(\frac{d}{b}\right)^{m_2} (1 - \hat{S}_{10})^{m_2} = 0$$

so that

$$\frac{\hat{S}_{10}^{m_1}}{(1 - \hat{S}_{10})^{m_2}} = \frac{\frac{1}{K} \left(\frac{d}{b}\right)^{m_2} \hat{G}_{20}^{n_2}}{\hat{G}_{10}^{n_1}} \quad (5.1)$$

From expression (5.1), we see that the reactant solid is zero when the product gas concentration is zero. From earlier results, we know that there are only two possibilities for  $\hat{G}_{20} = 0$ , namely in the *undisturbed* region where  $\hat{S}_{10} = 1$  and at the outer edge where  $\hat{S}_{10} = 0$ . Between the outer edge and the *undisturbed* region, from the transient analysis above, we see that the product gas is never zero. Thus from equation (5.1), we have  $\hat{S}_{10} = 0$  only at the outer edge implying that no moving boundary exists. This is shown in Figure (5a).

Case 2 :  $m_2 = 0, n_1, m_1, n_2$  non-zero

In this case, with  $m_2 = 0$ , the kinetics are independent of the product solid concentration and from equation (4.1), we have

$$\hat{S}_{10}^{m_1} = \frac{\hat{G}_{20}^{n_2}}{K \hat{G}_{10}^{n_1}} \quad (5.2)$$

Once again, with similar argument as in Case 1,  $\hat{S}_{10} = 0$  only at the outer edge, thus no moving boundary exists, see Figure (5b). It can be seen that for the region where  $\hat{S}_{10} = 1$ , we get

$$\hat{G}_{20}^{n_2} = K \hat{G}_{10}^{n_1}$$

Case 3 :  $m_1 = 0, n_1, n_2, m_2$  non-zero

For this case, the kinetics are independent of the reactant solid concentration and from equation (4.2), at  $x = 1$ , we have  $\hat{G}_{20} = 0$  and  $\hat{S}_{10} = 0$ . Thus for  $x \neq 1$ , substituting from equation (2.8), with  $m_1 = 0$ , gives

$$\left(\frac{d}{b}\right)^{m_2} (1 - \hat{S}_{10})^{m_2} = \frac{K \hat{G}_{10}^{n_1}}{\hat{G}_{20}^{n_2}}$$

Rearranging, we get

$$\hat{S}_{10} = 1 - \left[ \frac{\left(\frac{b}{d}\right)^{m_2} K \hat{G}_{10}^{n_1}}{\hat{G}_{20}^{n_2}} \right]^{\frac{1}{m_2}}$$

and  $\hat{S}_{10}(x \neq 1, t) = 0$  when

$$\hat{G}_{20}^{n_2} = \left(\frac{b}{d}\right)^{m_2} K \hat{G}_{10}^{n_1} \quad (5.3)$$

implying that a moving boundary exists as shown in Figure (5c).

Case 4 :  $m_1 = m_2 = 0, n_1, n_2$  non-zero

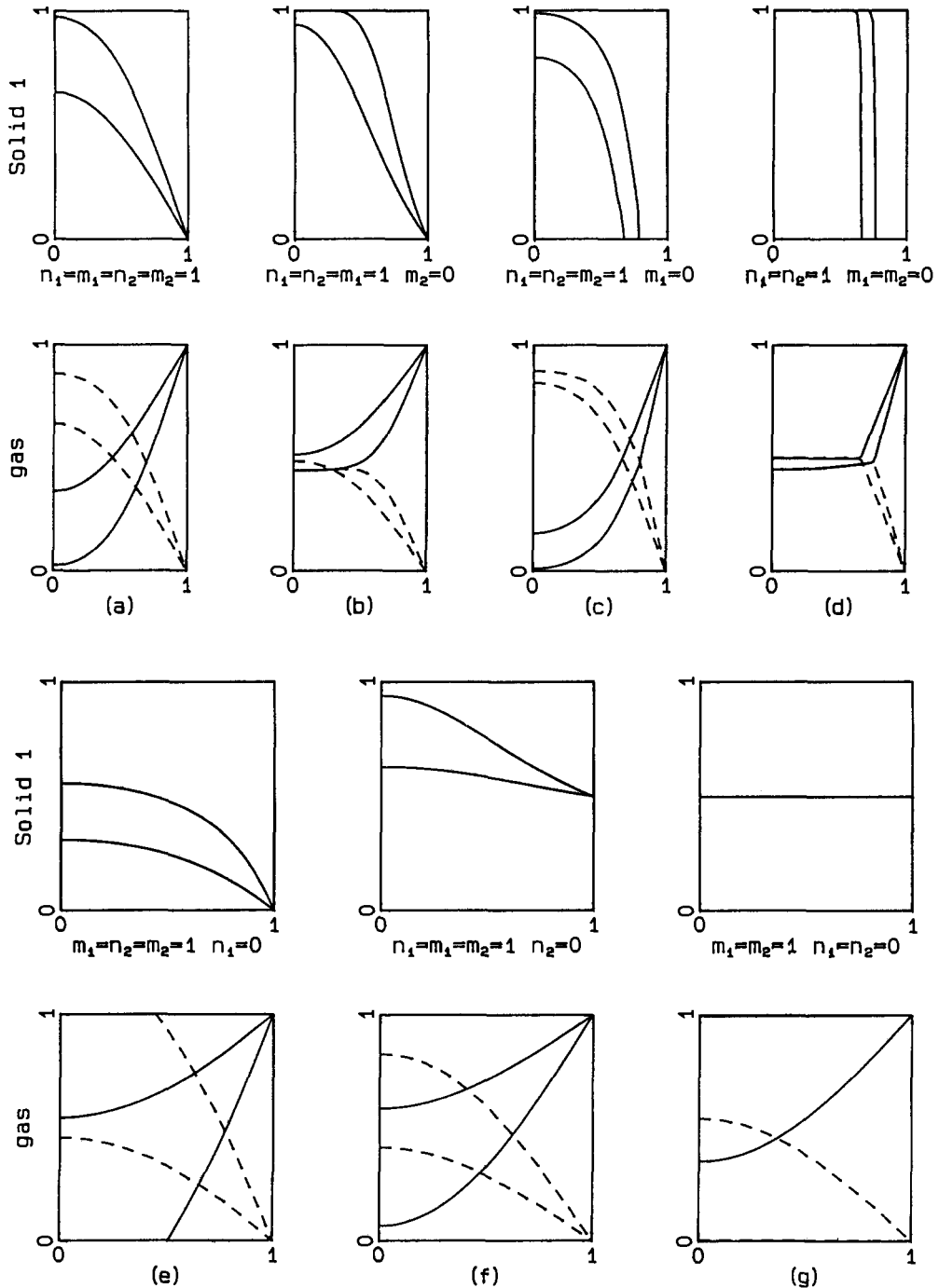


Fig. 5. Effect of the reaction orders for a slab geometry with  $\phi = 100, \psi = 0.1$  and  $t = 1, 3$  (\_\_\_\_\_ : Reactant solid or gas, - - - - : Product gas).

For this case, the reaction is independent of solid concentrations and from equation (4.1) we get

$$\hat{G}_{10}^{n_1} = \frac{1}{K} \hat{G}_{20}^{n_2} \quad (5.4)$$

We find that this relationship is not valid at the outer edge where  $x = 1$  as  $\hat{G}_{20} = 0$  and  $\hat{G}_{10} = 1$ . Thus the reactant solid has to be zero at the outer edge. Here the reactant solid is given by

$$S_1 = 1 - \int_0^t \hat{G}_{10}^{n_1} - \frac{1}{K} \hat{G}_{20}^{n_2} d\tau$$

When expression (5.4) is satisfied, the reactant solid remains at unity otherwise there exists a time such that  $S_1 = 0$ , implying that a moving boundary exists as shown in Figure (5d). From equation (5.4), as  $K \rightarrow \infty$ , we have  $\hat{G}_{10} = 0$  but if  $K$  is finite,  $\hat{G}_{10}$  takes on an equilibrium value in the region where  $\hat{S}_{10} = 1$ .

Case 5 :  $n_1 = 0, m_1, n_2, m_2$  non-zero

For this case, the kinetic form is independent of the reactant gas and we have

$$\frac{\hat{S}_{10}^{m_1}}{(1 - \hat{S}_{10})^{m_2}} = \frac{1}{K} \left(\frac{d}{b}\right)^{m_2} \hat{G}_{20}^{n_2} \quad (5.5)$$

With a similar argument to that in Case 1, since  $\hat{G}_{20}$  is zero at  $x = 1$  and in the *undisturbed* region,  $\hat{S}_{10}$  is zero only at the outer edge, see Figure (5e). Thus no moving boundary exists.

Case 6 :  $n_2 = 0, n_1, m_1, m_2$  non-zero

With  $n_2 = 0$ , the kinetics are independent of the product gas concentration, from equation (4.1) and rearranging, we have

$$\frac{\hat{S}_{20}^{m_2}}{\hat{S}_{10}^{m_1}} = K \hat{G}_{10}^{n_1} \quad (5.6)$$

and we can conclude that  $\hat{S}_{10}$  can never be zero, thus implying that there is no moving boundary as can be seen in Figure (5f).

Case 7 :  $n_2 = n_1 = 0, m_1, m_2$  non-zero

Lastly, when the kinetics are independent of both gases, we have

$$\frac{\hat{S}_{20}^{m_2}}{\hat{S}_{10}^{m_1}} = K \quad (5.7)$$

Once again, as in Case 6,  $\hat{S}_{10}$  can never be zero as shown in Figure (5g), implying that no moving boundary exists.

From the above analysis, we conclude that when the Thiele modulus is large, the criterion for which a shrinking core exists is only when the reversible reaction rate is independent of the reactant solid concentration, that is  $m_1 = 0$ . Thus, if the forward kinetics has even a slight dependence on the reactant solid concentration, the assumption of a shrinking core will not be appropriate (see case 2).

## 5. Estimates for conversion times

In this section, we analyse two particular cases, one where the parameters  $n_1, m_1, n_2$  and  $m_2$  are all non-zero and the other where the kinetics are independent of the reactant and product

solid concentrations. The former is interesting because of its generality and cases (2, 5–7), discussed in the previous section, are just modifications of this particular case. The latter case has been analysed by a number of research workers, McAdam *et al* [7] and Szekely *et al* [4], as it displays a shrinking core. Cases (3, 4) are of this shrinking core type. Conversion times for both cases are estimated and compared with that when the back reaction is neglected.

Conversion–Time Relationships

The amount of unreacted solid left in the particle,  $S_u$ , in dimensionless variables, is given by

$$S_u = \begin{cases} \int_0^1 S_1(\sigma, \tilde{t}) \, d\sigma, & \text{for a slab,} \\ \int_0^1 4\pi\sigma^2 S_1(\sigma, \tilde{t}) \, d\sigma, & \text{for a sphere.} \end{cases} \quad (6.1)$$

Another quantity which is quite often used as a measure of solid conversion is the fractional reduction,  $F$ , and this is given by

$$F = \begin{cases} 1 - S_u, & \text{for a slab,} \\ 1 - \frac{3}{4\pi} S_u, & \text{for a sphere.} \end{cases} \quad (6.2)$$

For the shrinking core case, using the approximation given by Do [5], we obtain

$$S_u = \begin{cases} X, & \text{for a slab,} \\ X^3, & \text{for a sphere.} \end{cases} \quad (6.3)$$

with the fractional reduction,  $F$ , given by

$$F = 1 - S_u \quad (6.4)$$

Here  $X$  is the position of the interface and is given by

$$X = 1 - (2\tilde{t})^{\frac{1}{2}} \quad \text{slab} \quad (6.5)$$

$$\frac{(1 - X^2)}{2} - \frac{(1 - X^3)}{3} = \tilde{t} \quad \text{sphere} \quad (6.6)$$

where  $\tilde{t}$  is the *slow* time scale, defined by  $\tilde{t} = \psi t$ , where  $\psi$  is assumed to be small.

For the case where a sharp interface is not obtained, Keady and Stakgold [21] have shown that the profile of the reactant solid remains convex and thus a good approximation for determining full conversion is when  $S_1(0, t_c) = 0$ , where  $t_c$  is the total conversion time.

We first express equations (2.1–2.4) in terms of the slow time scale  $\tilde{t}$ , and obtain

$$\psi\mu^2 \frac{\partial G_1}{\partial \tilde{t}} = \mu^2 \nabla^2 G_1 - f \quad (6.7)$$

$$\mu^2 \frac{\partial S_1}{\partial \tilde{t}} = -bf \quad (6.8)$$

$$\psi\mu^2 \frac{\partial G_2}{\partial \tilde{t}} = \delta\mu^2 \nabla^2 G_2 + cf \quad (6.9)$$

$$\mu^2 \frac{\partial S_2}{\partial \tilde{t}} = df \quad (6.10)$$

with initial and boundary conditions given by (2.5–2.7) with  $t$  replaced by  $\tilde{t}$ .

Utilising an expansion in  $\mu^2$  and assuming that  $\psi = O(\mu^2)$ , let

$$G_i = G_{i0} + \mu^2 G_{i1} + \dots$$

$$S_i = S_{i0} + \mu^2 S_{i1} + \dots$$

for  $i = 1, 2$ , and substitute into equations (6.7–6.10), we get

O(1)

$$G_{10}^{n_1} S_{10}^{m_1} - \frac{1}{K} G_{20}^{n_2} S_{20}^{m_2} = 0 \quad (6.11)$$

O( $\mu^2$ )

$$\nabla^2 G_{10} - f_1 = 0 \quad (6.12)$$

$$\frac{\partial S_{10}}{\partial \tilde{t}} = -b f_1 \quad (6.13)$$

$$\delta \nabla^2 G_{20} + c f_1 = 0 \quad (6.14)$$

$$\frac{\partial S_{20}}{\partial \tilde{t}} = d f_1 \quad (6.15)$$

subject to

$$\tilde{t} = 0, \quad G_{10} = G_{20} = S_{20} = 0, S_{10} = 1 \quad (6.16)$$

$$x = 0, \quad \frac{\partial G_{10}}{\partial x} = \frac{\partial G_{20}}{\partial x} = 0 \quad (6.17)$$

$$x = 1, \quad G_{10} = 1, G_{20} = 0 \quad (6.18)$$

#### CONSERVATION OF SOLIDS AND GASES

From the conservation of the solids, we know that

$$dS_{10} + bS_{20} = d \quad (6.19)$$

From equations (6.12) and (6.14), eliminating  $f_1$ , we have

$$\nabla^2(cG_{10} + \delta G_{20}) = 0 \quad (6.20)$$

and using the boundary conditions (6.17), (6.18) gives

$$cG_{10} + \delta G_{20} = c \quad (6.21)$$

which can be regarded as a *conservation of gases* condition.

Case A.  $n_1, m_1, n_2, m_2$  all non-zero.



In the general case, from equation (6.11), on this time scale, a pseudo-equilibrium exists where the forward and back reactions are approximately equal. Thus the reactant gas concentration is governed by the diffusion equation without the reaction term. The solution of this diffusion equation is given by

$$G_{10} = \begin{cases} 1 - \sum_{p=1}^{\infty} \frac{2}{\lambda_p} \sin \lambda_p \cos \lambda_p x e^{-\lambda_p^2 \tilde{t}}, & \text{for slab,} \\ 1 + \frac{1}{x} \sum_{p=1}^{\infty} \frac{2}{\lambda_p} \cos \lambda_p \sin \lambda_p x e^{-\lambda_p^2 \tilde{t}}, & \text{for sphere.} \end{cases} \quad (6.22)$$

where  $\lambda_p = (2p-1)\frac{\pi}{2}$  for slab and  $\lambda_p = p\pi$  for sphere,  $p = 1, 2, \dots$

The reactant solid is given from equation (6.11) and substituting from equations (6.19) and (6.21) we have,

$$\frac{S_{10}^{m_1}}{(1 - S_{10})^{m_2}} = \frac{1}{K} \left(\frac{d}{b}\right)^{m_2} \left(\frac{c}{\delta}\right)^{n_2} \frac{(1 - G_{10})^{n_2}}{G_{10}^{n_1}} \quad (6.23)$$

with  $S_{10} = 1$  when  $G_{10} = 0$ .

At the center of the particle,  $x = 0$ , we have

$$\frac{S_{10}^{m_1}(0, \tilde{t})}{[1 - S_{10}(0, \tilde{t})]^{m_2}} = \gamma \frac{[1 - G_{10}(0, \tilde{t})]^{n_2}}{G_{10}(0, \tilde{t})^{n_1}} \quad (6.24)$$

where

$$\gamma = \frac{1}{K} \left(\frac{d}{b}\right)^{m_2} \left(\frac{c}{\delta}\right)^{n_2}$$

We find that using only the first term of the summation series of equation (6.22), a simple expression providing good approximations can be obtained, that is

$$\frac{S_{10}^{m_1}(0, \tilde{t})}{[1 - S_{10}(0, \tilde{t})]^{m_2}} = \gamma \frac{\left[\frac{2}{\lambda_*^2} e^{-\lambda_*^2 \tilde{t}}\right]^{n_2}}{\left[1 - \frac{2}{\lambda_*^2} e^{-\lambda_*^2 \tilde{t}}\right]^{n_1}} \quad (6.25)$$

where

$$(\lambda_*, j) = \begin{cases} \left(\frac{\pi}{2}, 1\right), & \text{if slab,} \\ (\pi, 0), & \text{if sphere.} \end{cases}$$

If  $S_{10}(0, \tilde{t}) = \epsilon \ll 1$ , then  $(1 - \epsilon) \sim O(1)$ , and from equation (6.25), we have an expression for  $S_{10}(0, t_c)$  near full conversion, namely,

$$S_{10}^{m_1}(0, \tilde{t}) = \gamma \frac{\left[\frac{2}{\lambda_*^2} e^{-\lambda_*^2 \tilde{t}}\right]^{n_2}}{\left[1 - \frac{2}{\lambda_*^2} e^{-\lambda_*^2 \tilde{t}}\right]^{n_1}} \quad (6.26)$$

If  $n_1 = m_1 = n_2 = m_2$  and  $\gamma = 1$ , then from equation (6.23), we have

$$S_{10} = \frac{\delta}{c} G_{20} \quad \text{and} \quad G_{10} = \frac{d}{b} S_{20}$$

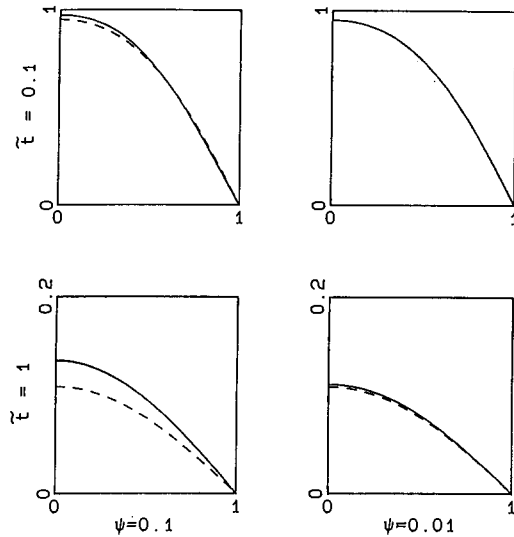


Fig. 6. Effect of the parameter  $\psi$ . Results obtained from a full numerical solution (—) for a slab geometry with  $\phi = 100$  and other parameters unity (this work : - - - - Results for the series method).

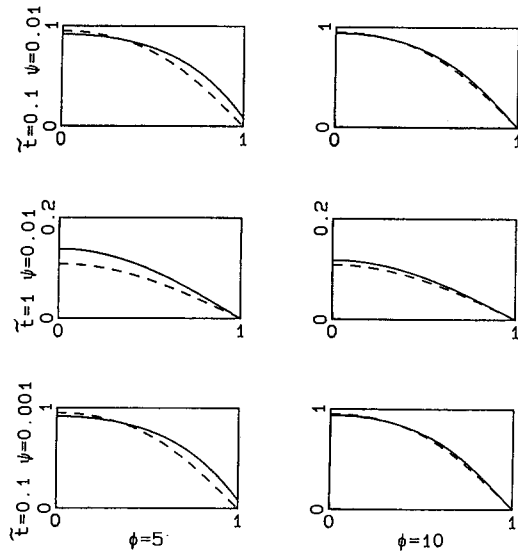


Fig. 7. Effect of the parameter  $\phi$ . Results obtained from a full numerical solution (—) for a slab geometry with other parameters unity (this work : - - - - Results for the series method).

Figures 6 and 7 show results for slab geometry with various values of the parameters. It can be seen that as  $\psi$  gets smaller, better results are obtained since we have made the assumption that  $\psi$  is small. It can also be concluded that for  $\phi \geq 10$  and  $\psi \leq 0.01$ , that is,  $\psi \sim \frac{1}{\phi^2}$ , good results are obtained. They are particularly good at longer times.

For this case, simple expressions for  $S_{10}(0, \tilde{t})$ ,  $S_u$  and  $F$  are available and are given by

$$S_{10}(0, \tilde{t}) = \frac{2}{\lambda_*^j} e^{-\lambda_*^2 \tilde{t}} \tag{6.27}$$

$$S_u = \frac{2}{\lambda_*^j} (4\pi)^{1-j} e^{-\lambda_*^2 \tilde{t}} \tag{6.28}$$

$$F = 1 - \left(\frac{3}{4\pi}\right)^{1-j} S_u \tag{6.29}$$

Table 1 shows the results for  $S_{10}(0, \tilde{t})$ ,  $S_u$  and  $F$  at time  $\tilde{t}$  together with the estimate of  $F$  obtained from the numerical solution of the full problem.

Table 1. Conversion estimates for a slab with  $\phi = 100$ ,  $\psi = 0.1$  and other parameters unity.

$\tilde{t}$	$S(0, \tilde{t})$	$S_u$	$F$	$F(num)$
1	0.107977044	0.068740321	0.9312597	0.9636575
2	0.009156990	0.005829521	0.9941705	0.9967979
3	0.000776558	0.000494372	0.9995056	0.9995883
4	0.000065856	0.000041925	0.9999581	0.9999813
5	0.000005585	0.000003555	0.9999964	0.9999686
6	0.000000470	0.000000302	0.9999997	0.9999901
7	0.000000040	0.000000026	1.0000000	0.9999995
8	0.000000003	0.000000002	1.0000000	0.9999995

It can be seen that, for this specific case the total dimensionless reduction time  $t_c$  for slab geometry is approximately 3. When the back reaction is neglected,  $t_c$  is approximately 0.5 as obtained from expression (6.5).

The results discussed above have by no means exhausted all the information regarding this very general case. Other simple expressions for conversion–time relationships can also be derived depending on the values of the reaction orders and  $\gamma$ .

**Case B :**  $m_1 = m_2 = 0, n_1, n_2 \neq 0$

Here the reaction kinetics is independent of the solid concentrations. As discussed in case (4) of the last section, this situation predicts the existence of an interface  $X$ . Then, for  $0 \leq x < X$

$$S_{10} \neq 0, G_{10} = G_{10}^*, G_{20} = G_{20}^*, G_{10}^{n_1} = \frac{1}{K} G_{20}^{n_2} \tag{6.30}$$

and for  $X < x \leq 1$ , we have  $S_{10} = 0$  with  $G_{10}$  satisfying the following,

$$\nabla^2 G_{10} = 0$$

subject to

$$\begin{aligned} x = X & \quad G_{10} = G_{10}^* \\ x = 1 & \quad G_{10} = 1 \end{aligned}$$

Solving for  $G_{10}$ , gives

$$G_{10} = \begin{cases} \frac{1}{1-X} [(x-X) + G_{10}^*(1-x)], & \text{for a slab,} \\ \frac{1}{x(1-X)} [(x-X) + G_{10}^*X(1-x)], & \text{for a sphere.} \end{cases} \tag{6.31}$$

$G_{20}$  is obtained from the conservation of gases condition, and we obtain

$$G_{20} = \begin{cases} \frac{G_{20}^*}{1-X}(1-x), & \text{for a slab,} \\ \frac{XG_{20}^*}{x(1-X)}(1-x), & \text{for a sphere.} \end{cases} \quad (6.32)$$

Here  $G_{10}^*$  and  $G_{20}^*$  are the equilibrium concentrations of  $G_{10}$  and  $G_{20}$  respectively. For the case of  $n_1 = n_2 = n$ , say, we have

$$G_{10}^* = \frac{c}{c + K^{\frac{1}{n}}\delta} \quad (6.33)$$

and

$$G_{20}^* = \frac{cK^{\frac{1}{n}}}{c + K^{\frac{1}{n}}\delta} = K^{\frac{1}{n}}G_{10}^*. \quad (6.34)$$

For the case of  $n_1 \neq n_2$ , numerical techniques have to be used to determine  $G_{10}^*$ , where

$$(G_{10}^*)^{n_1} = \frac{1}{K} \left(\frac{c}{\delta}\right)^{n_2} [1 - G_{10}^*]^{n_2} \quad (6.35)$$

and  $G_{20}^*$  is obtained from the conservation of gases condition. From equation (6.35), we see that when the back reaction is not neglected, we find that  $G_{10}^*$  cannot vanish. This confirms the statement by Szekely *et al* [4] that when back reactions are included, the equilibrium value of the reactant gas is non-zero.

The rate of movement of the position of the interface  $X$  is found to be balanced by the influx of the reactant gas, as discussed in Ishida and Wen [6] and Murray and Carey [17]. From equation (6.34), we have

$$X = 1 - (2(1 - G_{10}^*)\tilde{t})^{\frac{1}{2}} \quad \text{for a slab} \quad (6.36)$$

$$\frac{(1 - X^2)}{2} - \frac{(1 - X^3)}{3} = (1 - G_{10}^*)\tilde{t} \quad \text{for a sphere} \quad (6.37)$$

## 6. Conclusions

The study of gas–solid reactions is driven primarily by the fact they form the basis of many metallurgical processes such as ironmaking in blast furnaces or copper or nickel production in flash smelters. Approximate solutions to the reaction–diffusion equations which describe gas–solid reactions provide a deeper understanding of the rate–limiting processes. In addition, in large scale models of metallurgical processes it is often the case that tracing the degree of conversion of the reactants is the slowest step in the overall computational scheme. Accurate approximate solutions can reduce the computation time considerably by providing an alternative to the numerical solution of the full reaction–diffusion equations.

In Sections 3 and 4 of this paper we have analyzed the equations describing a gas–solid reaction using perturbation and series solution methods when the reaction is fast in comparison with the time for the reactant gas to diffuse. We show that at early times in the conversion process these provide excellent approximations.

One of the main simplifications made by researchers when examining gas-solid reactions is to assume the existence of a narrow reaction zone. In Section 5 we analyze this assumption under conditions where the reverse reaction is important. We show that, when power-law kinetics are applicable, this assumption holds only when the reaction rate is independent of the reactant solid concentration.

Obviously, the time for complete conversion of the reactant solid is of interest. In general, this cannot be estimated and a researcher must rely on the numerical solution of the full reaction-diffusion equations. However, under certain conditions, estimates of the conversion time can be found and Section 6 outlines several of these. They are extremely accurate and easy to compute and are based on the observation that, after a certain transient period, the behaviour of the system is governed by the form of the kinetic terms in the governing equations.

In summary, our results demonstrate that, within the framework of the gas-solid systems covered in this work, approximate methods provide a powerful investigative tool.

## Notation

### DIMENSIONAL QUANTITIES

$D_1, D_2$	Diffusion coefficients of reactant and product gas	$S_0$	Reactant initial solid concentration
$f'$	Total reaction rate	$S'_1, S'_2$	Reactant and product solid concentrations
$G_0$	Reactant bulk gas concentration	$\rho$	Porosity
$G'_1, G'_2$	Reactant and product gas concentrations	$t'$	Time variable
		$x'$	Spatial variable

### NONDIMENSIONAL QUANTITIES

$b, c, d$	Stoichiometric coefficients	$S_1, S_2$	Reactant and product solid concentrations
$f$	Total reaction rate	$S_0$	Reactant initial solid concentration
$G_1, G_2$	Reactant and product gas concentrations	$t$	Time variable
$G_0$	Reactant bulk gas concentration	$t^+$	Fast time variable
$K$	Equilibrium constant	$\bar{t}$	Slow time variable
$m_1, m_2$	Reaction orders of reactant and product solids	$t_c$	Total conversion time
$n_1, n_2$	Reaction orders of reactant and product gases	$x$	Spatial variable
		$X$	Position of interface

### Greek symbols

$\delta$	Ratio of diffusion coefficients of reactant and product gases	$\psi$	Ratio of initial reactant gas to solid
$\phi$	Thiele modulus	$\mu$	Inverse Thiele modulus

## References

1. P.A. Ramachandran and L.K. Doraiswamy, Modelling of non-catalytic gas-solid reactions. *A.I.Ch.E. J.* 28 (1982) 881-899.
2. B.S. Sampath and R. Hughes, A review of mathematical models in single particle gas-solid noncatalytic reactions. *Chem. Eng. (London)*. 278 (1973) 485-497.
3. O. Levenspiel, *Chemical Reaction Engineering*, Wiley, New York (1973).
4. J. Szekeley, J.W. Evans and H.Y. Sohn, *Gas-Solid Reactions.*, New York: Academic Press, (1976).
5. D.D. Do, On the validity of the shrinking core model in non-catalytic gas-solid reactions. *Chem. Eng. Sci.* 37 (1982) 1477-1481.
6. M. Ishida and C.Y. Wen, Comparison of kinetic and diffusional model for gas-solid reactions. *A.I.Ch.E. J.* 14 (1968) 311-317.

7. G.D. McAdam, A. McNabb and E. Bradford, Experimental support for a coupled diffusion model of iron-oxide reduction. *Ironmaking and Steelmaking* 15 (1988) 219–227.
8. M.D. Borghi, J.C. Dunn and K.B. Bischoff, A technique for solution of the equations for fluid-solid reaction with diffusion, *Chem. Eng. Sci.* 31 (1976) 1065–1069.
9. M.P. Dudukovic A note on gas–solid noncatalytic reactions, *A.I.Ch.E. J.* 22 (1976) 945–947.
10. I. Stakgold and A. McNabb, Conversion estimates for gas-solid reactions. *Mathematical Modelling* 5 (1984) 325–330.
11. A. Aziz and T.Y. Na, *Perturbation Methods in Heat Transfer*, New York: Hemisphere Publishing Corporation, (1984).
12. A.K. Kapila, *Asymptotic Treatment of Chemically Reacting Systems*, Applicable Mathematics Series, Boston: Pitman Publishing Pty. Ltd., (1983).
13. H.S. Carslaw and J.C. Jaeger, *Conduction of Heat in Solids*, Oxford: Oxford University Press, (1965).
14. T.Y. Na, *Computational Methods in Engineering Boundary Value Problems, Chapter 2*, New York: Academic Press, (1979).
15. Y.H. Chan and D.L.S. McElwain, Conversion estimates for gas–solid reactions : Kinetics of arbitrary power-law type. *Mathl. Comput. Modelling* 17, No. 1 (1993) 95–103.
16. K.B. Bischoff, Further comments on the pseudo steady state approximation for moving boundary diffusion problems. *Chem. Eng. Sci.* 20 (1965) 783–784.
17. P. Murray and G.F. Carey, Finite element analysis of diffusion with reaction at a boundary. *J. Comp. Phys.* 74 (1988) 440–455.
18. G.F. Carey and P. Murray, Perturbation analysis of the shrinking core. *Chem. Eng. Sci.* 44 (1989) 979–983.
19. S.K. Bhatia, Perturbation analysis of gas–solid reactions I. Solid of low initial permeability. *Chem. Eng. Sci.* 46 (1991a) 173–182.
20. S.K. Bhatia, Perturbation analysis of gas–solid reactions II. Reduction to the diffusion–controlled shrinking core. *Chem. Eng. Sci.* 46 (1991b) 1465–1474.
21. G. Keady and I. Stakgold, *Some Geometric Properties of Solids in Combustion*, In: *Symposia Mathematica, XXX* 137 in *Geometry of Solutions to Partial Differential Equations*, London: Academic Press, (1989).